analytical chemistry

Article

pubs.acs.org/ac

Label-Free Detection of Carbohydrate–Protein Interactions Using Nanoscale Field-Effect Transistor Biosensors

Guo-Jun Zhang,*[,†,‡] Min Joon Huang,[‡] Jun'An Jason Ang,[‡] Qunfeng Yao,[†] and Yong Ning*[,†]

[†]School of Laboratory Medicine, Hubei University of Chinese Medicine, 1 Huangjia Lake West Road, Wuhan 430065, China

[‡]Institute of Microelectronics, A*STAR, Agency for Science, Technology and Research, 11 Science Park Road, Singapore 117685

Supporting Information

ABSTRACT: Carbohydrate–protein interactions play a significant role in cell communication, cell adhesion, cell trafficking, and immune responses. Many efforts have been made to demonstrate detection of carbohydrate–protein interactions. However, the existing methods are still tedious and expensive. Therefore, the detection of carbohydrate–protein interactions is of great significance, and new, efficient methods are required for fast and sensitive recognition testing. In this report, we, for the first time, developed the silicon nanowire (SiNW)-based biosensor capable of label-free electrical detection of carbohydrate–protein interactions with high selectivity and sensitivity by covalently immobilizing unmodified carbohydrates on the sensor surface. We fabricated new SiNW sensor chips with more SiNW arrays for potential detection of multiple analytes. In order to realize the immobilization of the unmodified carbohydrates on the SiNW surface, we used X-ray photoelectron spectra and fluorescence microscopy to verify the successful surface functionalization on the silicon surface. Furthermore, we demonstrated real-time detection of carbohydrate–protein interactions using the carbohydrate-modified SiNW sensor chips. The results show good specificity between galactose–lectin EC and mannose–Con A, which is in good agreement with that reported previously. Finally, the results also show that we are able to use the galactose-modified SiNW biosensor to detect lectin EC as low as 100 fg/mL, which is 4 orders of magnitude lower than that reported by other technologies. We believe that the developed SiNW biosensor paves a novel way for studying carbohydrate–protein interactions.

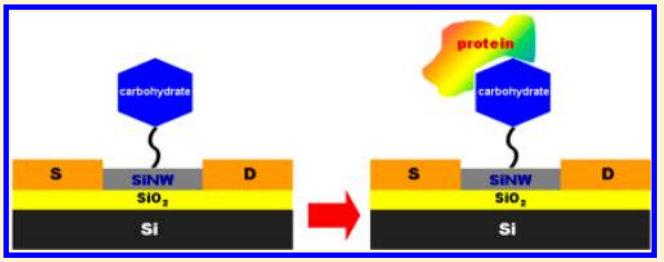

Carbohydrates are important components of the cell membrane and specifically recognized by other molecules like proteins.[1] Carbohydrate–protein interactions play a significant role in biological functions such as cell communication, cell adhesion, cell trafficking, and immune responses.[2,3] A better understanding of carbohydrate–protein interactions would help elucidate intercellular signaling pathways, possibly leading to new tools for diagnosis and therapeutics.[4−6] To this end, detection of carbohydrate–protein interactions is of great significance, and new, efficient methods are required for fast and sensitive recognition testing.

Lectins are known as sugar-binding proteins, and studies on lectin–protein interactions have recently received increased attention. Since binding of lectin–protein interactions is weaker than that of protein–protein interactions, several new methods for understanding lectin–protein interactions have been employed including carbohydrate microarray,[7−9] electrochemical assay,[10] surface plasmon resonance (SPR),[11,12] and carbon nanotube-based nanoelectronic detection.[13] Microarray-based technologies as powerful tools are widely used in determining functions of nucleic acids and proteins. Recently carbohydrate microarrays were exploited for rapidly studying the binding profile of carbohydrate-binding proteins.[7] Zhou and Zhou developed a convenient and efficient method to prepare oligosaccharide microarrays on aminooxyacetyl-functionalized glass surface for carbohydrate–protein interactions.[8] Gao et al. proposed a gold nanoparticle-based instead of a conventional fluorescent dye-based carbohydrate microarray for highly sensitive and selective monitoring of carbohydrate–protein interactions, which shows great potential as a high-throughput tool for glycoproteome screening.[9] Zhang et al. reported a novel lectin-based electrochemical biosensor for highly sensitive and selective detection of cancer-associated glycan expression on living cells, which may greatly facilitate the medical diagnosis and treatment in the early process of cancer.[10] SPR as an emerging technique is being used to study carbohydrate–protein interactions. Linman et al. used SPR to probe lectin–carbohydrate interactions in a quantitative manner based on a new sensing surface of biotinylated sialosides.[11] Beccati et al. investigated SPR studies of carbohydrate–protein interactions by labeling low-molecular-mass saccharides with the PtCl (NCN-R) aglycon, which is capable of enhancing the SPR response.[12] However, the existing methods for studying carbohydrate–protein interactions are still time-consuming, requiring expensive instrumentation and technical expertise. Recently, Vedala et al. used single-walled carbon nanotube

Received: December 17, 2012
Accepted: April 11, 2013
Published: April 11, 2013

   dx.doi.org/10.1021/ac3036525 | *Anal. Chem.* 2013, 85, 4392–4397

field-effect transistor (FET) devices to probe carbohydrate−lectin interactions, showing a novel nanodevice platform for highly selective detection of interactions between glycoconjugate and bacterial lectin.[13]

Compared to the carbon nanotube-based FET biosensor, the silicon nanowire (SiNW)-based FET biosensor has particularly attracted much attention because of its capabilities in detecting biomolecules in a sensitive fashion, coupled to its manufacturability for mass production, benefiting from mature semiconductor fabrication. Examples have demonstrated the applications of the SiNW-based FET biosensor for the detection of nucleic acids,[14−25] proteins,[26−31] viruses,[32] protein−DNA interactions,[33,34] and cells.[35−37] In addition to the SiNW-based FET biosensor, carbon nanotube and graphene based FET biosensors have also been utilized for successful detection of protein molecules.[38−40] In particular, the SiNW FET biosensor has been utilized in applications for disease-related diagnostics.[41] Nevertheless, the application of the SiNW-based FET biosensor for carbohydrate−protein interactions has not been yet discovered.

In this work, we, for the first time, developed the SiNW-based biosensor capable of label-free electrical detection of carbohydrate−protein interactions with high specificity and sensitivity by covalently immobilizing unmodified carbohydrates on the sensor surface. Prior to the immobilization, the SiNW sensor chip was fabricated by a top-down approach. To avoid modifying carbohydrates with active groups, we employed covalent immobilization of unmodified carbohydrates on the SiNW surface by formation of an oxime bond through amine groups modified with 3-aminopropyltriethoxysilane, and subsequently aminooxyacetyl groups introduced with Boc-aminooxyacetic acid. X-ray photoelectron spectra (XPS) and fluorescence microscope were employed to demonstrate the successful surface chemistry for immobilization of carbohydrates and binding of carbohydrate−protein on the silicon surface. The label-free electrical detection of carbohydrate−protein interactions was then carried out by the carbohydrate-modified SiNW biosensor.

EXPERIMENTAL SECTION

Materials. Galactose, succinic anhydride, 1-ethyl-3-(3-dimethyllaminopropylcarbodiimide) (EDC), *N*-hydroxysuccinimide (NHS), 3-aminopropyltriethoxysilane (APTES, 99%), and bovine serum albumin (BSA) were purchased from Sigma-Aldrich. Mannose, concanavalin A from *Canavalia ensiformis* (Con A), lectin from *Erythrina cristagalli* (lectin EC), and lectin from *E. cristagalli* TRITC-labeled were purchased from Sigma. Boc-aminooxyacetic acid was purchase from Aldrich.

Fabrication of the SiNW Biosensor. The SiNW biosensor chip was fabricated using n-doped silicon-on-insulator (SOI) substrate as previously reported.[28] Eight inch SOI wafers with 700 Å silicon and 1450 Å buried oxide layers were used for silicon nanowire fabrication. Silicon fins of ∼100 nm widths were patterned using deep ultraviolet lithography and reactive-ion etching. An oxidation at 875 °C was further employed to scale down the nanowire width to ∼80 nm. Next, a phosphorus implantation was done at 30 keV for a dose of 5×10^{13} cm^{-2}, and activated at 1000 °C for 30 s in N_2. A 3900 Å of high-density plasma oxide was used for nanowire passivation, and contact holes were opened at both ends of the nanowires. A high-dose (5×10^{15} cm^{-2}) phosphorus implantation and activation was conducted to obtain n+ regions. Ohmic contacts were realized after TaN/AlSiCu metallization and annealing at 420 °C for 30 min. Finally, 1000 Å nitride/15 000 Å oxide/2000 Å nitride passivation layers were deposited to protect the metal lines, leaving the metal pads and active nanowire sensor areas exposed. The nanowires were released by dry etching of the nitride/oxide/nitride passivation layers followed by wet etching of the remaining SiO_2 using diluted HF. The devices were stored in a desiccator cabinet for 5 days, which allowed native oxide growth on the nanowire surface.

Functionalization of the Aminooxyacetyl-Terminated SiNW Surface. As published previously,[23] a similar chemistry was employed to terminate the SiNW surface with amine groups on the SiNW surface using APTES in the first step. The SiNW chip was immersed into 2% APTES in a mixture of ethanol/water (95%/5%, v/v) for 2 h. The chip was washed with absolute ethanol for three times and blow-dried. The chip was then immersed in 1 mM Boc-aminooxyacetic acid in phosphate-buffered saline (PBS) mixed with EDC and NHS for 2.5 h. To remove the BOC group, the chip was rinsed with water and immersed into 2 M HCl/acetic acid for 2 h. The chip was washed with ethanol, water, then blow-dried.

Immobilization of Carbohydrate. It was found that pH of the buffer solution used, reaction time, and temperature for incubation affected the efficiency of the carbohydrate immobilization. As reported by the other group,[42] optimal conditions like pH, reaction temperature, and time were conducted in this work. In brief, 30 μM carbohydrate in PBS (pH 5) was incubated with the SiNW biosensor chip in a humidified environment at 50 °C overnight. After which, the chip was washed with PBS containing 0.1% Tween-20. A solution of 10 mM succinic anhydride in *N*,*N*-dimethylformamide (DMF) was used to inactivate the unreacted aminooxyacetyl groups on the SiNW surface. To minimize adsorption of protein, the SiNW chip was further treated with 1% BSA in PBS.

Electrical Measurement. Electrical measurements of SiNW conductances were conducted by an Alessi REL-6100 probe station (Cascade Microtech, Beaverton, OR) incorporated with an HP parameter analyzer (HP-4155A). A short pulse voltage of 0.1 V was applied to the SiNW device, and the current through the SiNW was measured. To make a fluidic exchange, an acrylic well was employed according to the SiNW chip size. The well was localized on the chip surface covering the SiNW clusters, which allowed the fluid supply and return. The nanowire conductance was recorded as a function of time while the carbohydrate-functionalized SiNW chip was exposed to the proteins. As described previously,[28] 0.01× PBS buffer solution (pH 7.4) which has a long Debye length was used in the experiment.

On the basis of the data sequence of lectin EC,[43] we could calculate the pI of the protein as 5.0 using a software. As known, the pI of Con A is between 4.5 and 5.5. Thus, theoretically speaking, knowing that the pH of the buffer is 7.4 and the pI is approximately 5.0, we can denote that the charge of both proteins is negative in 0.01× PBS.

X-ray Photoelectron Spectroscopy. X-ray photoelectron spectra were obtained on a PHI Quantera SXM scanning X-ray microprobe (ULVAC-PHI, Inc., Japan) using monochromatic Al Kα X-rays (1486.6 eV). Pass energies of 224 and 55 eV were used for the survey scan and high-resolution (narrow) scan, respectively. The spot size was 200 μm. The sample surface was tilted at 45° with respect to the analyzer detector.

Fluorescence Microscopy. The fluorescence microscopy was performed using an Olympus BX61 epi-fluorescence

dx.doi.org/10.1021/ac3036525 | *Anal. Chem.* 2013, 85, 4392−4397

microscope equipped with a color cooled CCD camera SPOT-RT Slider (Diagnostic Instruments, U.S.A.), a 100 W HBO bulb, and Olympus fluorescence filter sets (U-MWU2, U-MWB2, U-MF2).

RESULTS AND DISCUSSION

Design of the SiNW Sensor Chip. In this work, the SiNW biosensors for detection of carbohydrate−protein interactions were demonstrated by covalently immobilizing unmodified carbohydrates on the SiNW sensor surface. Prior to the immobilization, the SiNW sensor chip was fabricated. As illustrated in Figure 1a, covalent immobilization of unmodified

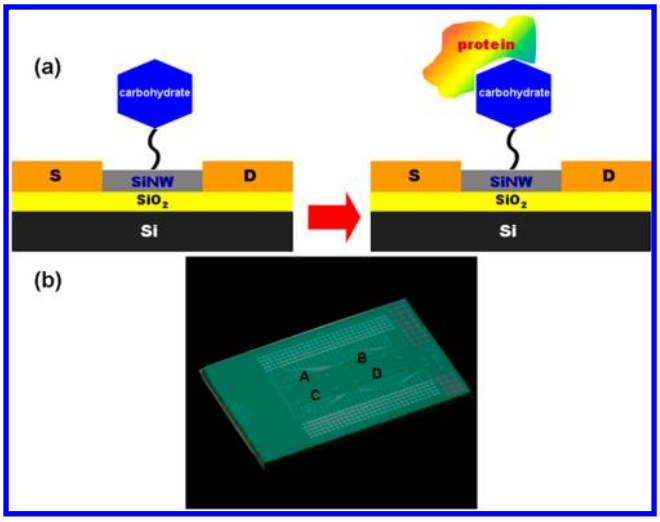

Figure 1. (a) Schematic diagram of the SiNW biosensor for label-free detection of carbohydrate−protein interactions. (b) Optical image of a SiNW sensor chip with four clusters.

carbohydrates on the SiNW surface by formation of an oxime bond through amine groups modified with 3-aminopropyltriethoxysilane is carried out. Subsequently, aminooxyacetyl groups are introduced with Boc-aminooxyacetic acid. The immobilization of carbohydrates is finally realized on the SiNW surface. The label-free electrical detection of carbohydrate−protein interactions is then carried out by the carbohydrate-modified SiNW biosensor.

The SiNW sensor chips were fabricated through conventional optical lithography as reported previously including the processes like etching and oxidation.[28] The sensor arrays thus are fully compatible with CMOS technology. In this work, a different SiNW chip layout with 255 nanowires in 51 different clusters was designed to produce more NW array sensors for detection. The fabrication process is similar to that reported before, in addition to the different format. Figure 1b shows an optical image of the new SiNW chip. A total of 255 individual nanowires were fabricated in four groups, A, B, C and D, respectively. In group A, B, and C, each has 12 clusters (five nanowires in one cluster) with a distance of 300 μm in between. Differently, group D has 15 nanowire clusters with the same pitch.

X-ray Photoelectron Spectroscopy Characterization of Carbohydrate Immobilization on the Silicon Surface. Efficient immobilization of carbohydrate on the SiNW surface is playing a significant role for successful preparation of the SiNW biosensor for study of carbohydrate−protein interactions. Most methods involve immobilization of the chemically modified carbohydrates onto the properly derivatized surfaces. In order to obtain the functionalized sugar molecules, multistep synthesis procedures are required, which remains time-consuming and costly. Immobilization methods that employ unmodified carbohydrates have been reported in an attempt to avoid the use of the functionalized sugar molecules, of which covalent attachment of carbohydrates to the hydrazide- and aminooxy-derivatized surface is simple and site-specific. Zhou and Zhou reported that an oxime chemistry was utilized to immobilize the carbohydrates to the glass surface by functionalizing the surface with aminooxyacetyl groups.[8] The method allowed an ease of formation and a good stability for high immobilization efficiency due to the oxime linkage.

Different from the above-mentioned method, we developed a new method for covalently immobilizing unmodified carbohydrate on the silicon surface. As diagramed in Figure 2, the

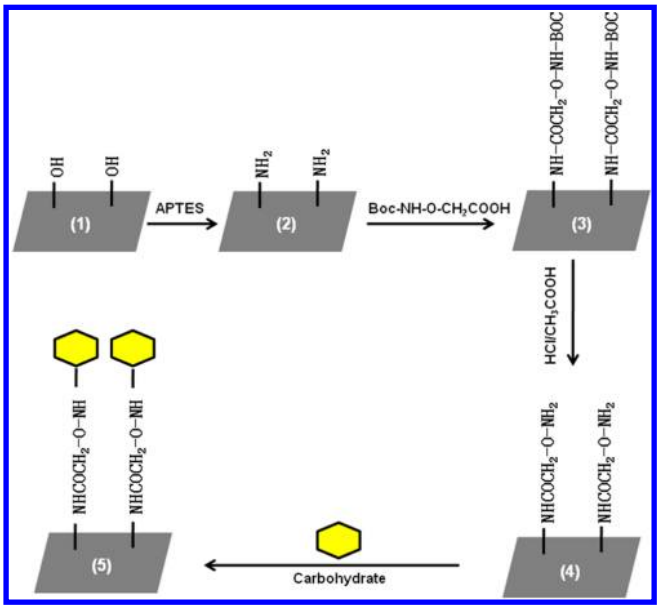

Figure 2. Surface functionalization of unmodified carbohydrate on the silicon surface via oxime bonding.

silicon surface is functionalized with APTES to generate an amine group. The amine group is then coupled to the carboxyl group of Boc-aminooxyacetic acid in the presence of EDC and NHS followed by treatment of acid to produce the aminooxyacetyl group. Finally, the carbohydrate is efficiently immobilized on the silicon surface via oxime bonding. In order to characterize the stepwise functionalization procedure in the work, the surface chemistry used in the study was verified by XPS by using bare silicon substrate rather than the silicon nanowire surface because such a characterization cannot be carried out on the nanoscale structure. Although the C1s and O1s appear in each step, in practice XPS does not distinguish between all the different carbons and oxygens because the silicon surface is always adsorbed with water molecules. However, the N1s element is indicative because various bonds between N and other elements like C and O are formed. Figure 3 shows XPS spectra for nitrogen (1s) in every step, respectively. No N1s is seen in Figure 3a, meaning that the silicon surface was not modified and only covered with hydroxyl groups. After treatment with APTES, the surface was functionalized with amine groups. Subsequently, an obvious N1s peak was obtained at 398.4 eV as shown in Figure 3b.

dx.doi.org/10.1021/ac3036525 | Anal. Chem. 2013, 85, 4392−4397

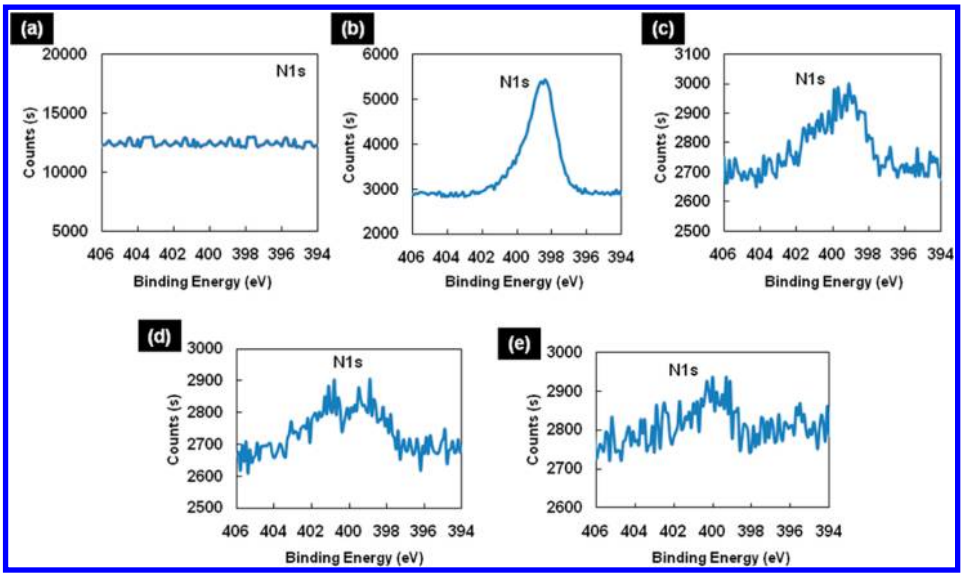

Figure 3. XPS spectra for nitrogen (1s) in every step of surface functionalization of unmodified carbohydrate on the silicon surface: (a) bare silicon surface; (b) APTES-modified surface; (c) Boc-aminooxyacetic acid treated surface; (d) aminooxyacetyl group modified surface after treatment with acid; (e) carbohydrate-modified surface.

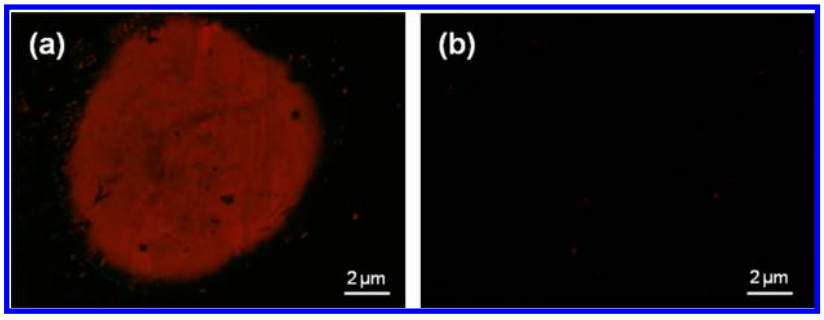

Figure 4. Fluorescent illustration of carbohydrate–protein binding on the silicon surface: (a) binding of TRITC-labeled lectin EC with the immobilized galactose; (b) binding of TRITC-labeled lectin EC with the immobilized mannose.

Figure 3c illustrates two N1s peaks, at 399.1 and 399.7 eV, respectively, which are attributed to an amido bond formed between the amine group and carboxylic group and an aminooxy bond introduced by the Boc-aminooxyacetic acid. The free aminooxyacetyl group was then observed after the BOC group was removed by using HCl/acetic acid. As a result, a strong N1s peak at 400.8 eV is seen in Figure 3d, indicating that the free amine group appeared again. The other N1s peak is also obvious at 398.9 eV, which is attributed to the amido group. After carbohydrate immobilization, Figure 3e shows two N1s peaks at 399.3 and 400.0 eV, corresponding to amido and aminooxy groups, respectively. From the XPS data, it is clear that the stepwise functionalization takes place as anticipated, and the carbohydrate has successfully been immobilized on the silicon surface.

Fluorescent Verification of Carbohydrate–Protein Binding on the Silicon Surface. To verify the subsequent binding of carbohydrate–protein using the oxime chemistry, fluorescence was employed to illustrate the event on the silicon surface. The aim of using fluorescence was to achieve and obtain evidence behind the concept that the galactose probe has been immobilized on the aminooxyacetyl-functionalized silicon surface. Knowing that lectin EC will specifically bind to galactose, a fluorescently (TRITC) labeled lectin EC is applied on the chip, and the chip is then observed under the fluorescence microscope after incubation. As illustrated in Figure 4a, a bright spot was observed under the fluorescence microscope, hence implying that the probe has been successfully immobilized on the surface of the silicon surface and the binding has taken place subsequently. To investigate the specificity of the binding event, mannose was immobilized on the silicon surface using the same chemistry; the TRITC-labeled lectin EC was used again. Negligible fluorescence was seen on the substrate (Figure 4b), indicating that lectin EC is not specific to mannose. The fluorescence microscope demonstrates the successful surface chemistry for immobilization of carbohydrates on the silicon surface and the specific binding of carbohydrate–protein.

Specificity of Carbohydrate–Protein Interactions. Specificity of carbohydrate–protein interactions was verified by the carbohydrate-modified SiNW biosensor. Real-time response of lectin EC and Con A to the galactose- and mannose-modified SiNW biosensors, respectively, as function of time was achieved. As shown in Figure 5a, when BSA and Con A were applied to the galactose-modified SiNW biosensor, a negligible response was obtained, whereas an obvious current drop was clearly seen when lectin EC was applied to the galactose-modified SiNW biosensor. This means that galactose is nonspecific to BSA and Con A, but specific to lectin EC. Similarly, as shown in Figure 5b, when Con A was injected to

dx.doi.org/10.1021/ac3036525 | *Anal. Chem.* 2013, 85, 4392–4397

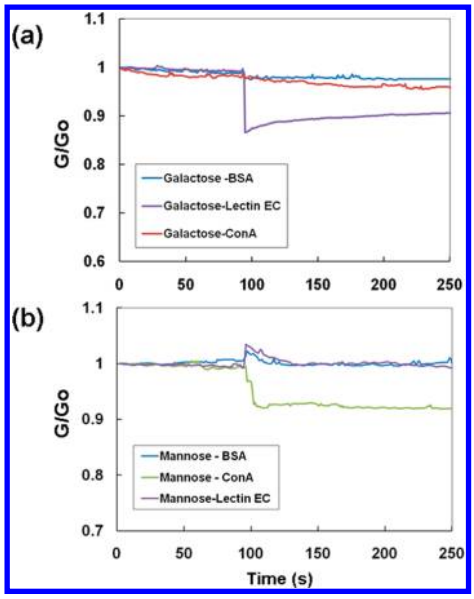

Figure 5. Real-time response of the carbohydrate-modified SiNW biosensor to the corresponding proteins: (a) specificity of galactose–lectin EC binding; (b) specificity of mannose–Con A binding.

the mannose-modified SiNW biosensor, a response was clearly observed. However, a negligible response was observed while BSA and lectin EC were applied to the mannose-modified sensor surface, respectively. The results indicate that the carbohydrate-modified SiNW biosensor shows satisfactory specificity to the corresponding protein, which is in good agreement with those reported earlier.[8]

Sensitivity of Carbohydrate–Protein Interactions. The limit of detection is of great significance for the detection of carbohydrate–protein interactions. Various techniques have demonstrated the different detection limits for different lectin detections, such as Au-nanoparticle-based colorimetric assay (64 nM),[44] SPR (41 nM),[11] electrochemical impedance spectroscopy (5 nM),[45] and optical microarray (~8 ng/mL).[8] Recently, Vedala et al. reported that a glycoconjugate-functionalized single-walled carbon nanotube (SWCNT) FET device was capable of detecting 2 nM lectin, in which the SWCNT network was used in the channel between the source and drain.[13] Very recently, Gruber et al. reported a cantilever-based array sensor, which could selectively and sensitively analyze carbohydrate–protein interactions and detect picomolar concentration of carbohydrate-binding protein (91 pM cynanovirin-N).[46]

The sensitive detection of carbohydrate–protein interactions was then carried out by the galactose-modified SiNW biosensor to lectin EC. Various concentrations of lectin EC were prepared by dissolving lectin EC in 0.01× PBS buffer and applying to the galactose-modified SiNW biosensor. As seen in Figure 6, the real-time response of conductance upon injection of varying concentrations of lectin EC from 1 ng/mL to 10 fg/mL was observed. The addition of blank buffer (0.01× PBS) without lectin EC did not result in a current change, showing that the SiNW biosensor is stable. The change in conductance decreased along with the decrease of the concentrations of lectin EC. It was found that 100 fg/mL lectin EC was detected by the galactose-modified SiNW biosensors, which was the highest sensitivity compared to those developed by other technologies.

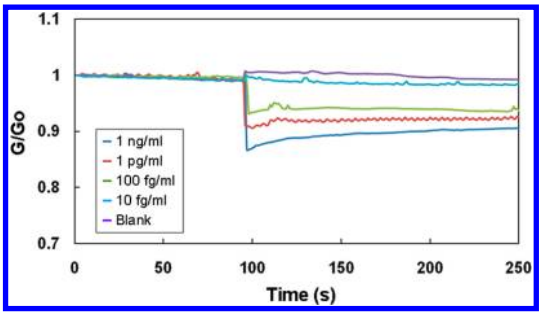

Figure 6. Real-time detection of lectin EC with the galactose-modified SiNW biosensor.

The state-steady detection of interaction of lectin EC and galactose was carried out by measuring the SiNW working current–voltage (I–V) curves after galactose was immobilized onto the SiNW surface and after lectin EC was bound to the immobilized galactose, respectively. Supporting Information Figure S2 illustrates the SiNW working I–V curves before and after 1 ng/mL concentration of lectin EC was bound to the galactose-functionalized SiNW surface. It was found that the SiNW current dropped after the negative charges of lectin EC were introduced to the SiNW surface, which is in good agreement with the results of the real-time detection as mentioned above. The results also show how the SiNW FET biosensor operates at the immobilization of carbohydrate and the interaction between immobilized carbohydrate and protein.

In comparison with other technologies, our technique offers a distinctive advantage in having a very low detection limit for detection of carbohydrate–protein interactions. This can be explained by utilization of a small size of SiNW as the sensing element, resulting in large surface-to-volume ratio. The detection sensitivity achieved in the work compares well to the best reported sensitivities for antibody–antigen assay that range in the low subpicogram per milliliter regime.[28,30,31]

Reproducibility. The reproducibility of the assay was evaluated by utilizing the galactose-modified SiNW for detection of lectin EC. The relative standard deviation (RSD) was calculated to be <15% on different SiNW sensors, indicating a satisfactory reproducibility for identification of carbohydrate–protein interactions.

■ CONCLUSIONS

In conclusion, an approach to covalently attaching unmodified carbohydrate to the SiNW surface and the carbohydrate-modified SiNW biosensor for electrical detection of carbohydrate–protein interactions has been, for the first time, demonstrated. A simple and efficient method to prepare unmodified carbohydrates to be immobilized on amino-oxyacetyl-functionalized SiNW surface by oxime bonding formation has been carried out. The carbohydrate molecules have been proven to be immobilized on the silicon surface successfully by XPS and fluorescent microscopy. The SiNW biosensors show not only good specificity of carbohydrate–protein interactions but also high sensitivity of galactose–lectin EC interactions. This study indicates that the developed SiNW biosensors are a robust, sensitive, and label-free means to analyze carbohydrate–protein interactions and to detect subpicogram per milliliter concentrations of carbohydrate-binding proteins.

■ ASSOCIATED CONTENT

Supporting Information

Additional information as noted in text. This material is available free of charge via the Internet at http://pubs.acs.org.

■ AUTHOR INFORMATION

Corresponding Author

*Phone: +86-27-68890259. Fax: +86-27-68890071. E-mail: zhanggj@hbtcm.edu.cn (G.-J.Z.); ningyong128@163.com (Y.N.).

Notes

The authors declare no competing financial interest.

■ ACKNOWLEDGMENTS

The authors acknowledge Ms. Dao Thuy Khanh Linh Kathy at the Data Storage Institute in Singapore for her assistance with XPS spectra.

■ REFERENCES

(1) Dwek, R. A. *Chem. Rev.* **1996**, *96*, 683−720.
(2) Varki, A. *Nature* **2007**, *446*, 1023−1029.
(3) Ohtsubo, K.; Marth, J. D. *Cell* **2006**, *126*, 855−867.
(4) Ratner, D. M.; Adams, E. W.; Disney, M. D.; Seeberger, P. H. *ChemBioChem* **2004**, *5*, 1375−1383.
(5) Seeberger, P. H.; Werz, D. B. *Nat. Rev. Drug Discovery* **2005**, *4*, 751−763.
(6) Werz, D. B.; Seeberger, P. H. *Chem.—Eur. J.* **2005**, *11*, 3194−3206.
(7) De Paz, J. L.; Seeberger, P. H. *QSAR Comb. Sci.* **2006**, *25*, 1027−1032.
(8) Zhou, X. C.; Zhou, J. Z. *Biosens. Bioelectron.* **2006**, *21*, 1451−1458.
(9) Gao, J. Q.; Liu, D. J.; Wang, Z. X. *Anal. Chem.* **2008**, *80*, 8822−8827.
(10) Zhang, X.; Teng, Y.; Fu, Y.; Xu, L.; Zhang, S.; He, B.; Wang, C.; Zhang, W. *Anal. Chem.* **2010**, *82*, 9455−9460.
(11) Linman, M. J.; Taylor, J. D.; Yu, H.; Chen, X.; Cheng, Q. *Anal. Chem.* **2008**, *80*, 4007−4013.
(12) Beccati, D.; Halkes, K. M.; Batema, G. D.; Guillena, G.; Carvalho de Souza, A.; van Koten, G.; Kamerling, J. P. *ChemBioChem* **2005**, *6*, 1196−1203.
(13) Vedala, H.; Chen, Y.; Cecioni, S.; Imberty, A.; Vidal, S.; Star, A. *Nano Lett.* **2011**, *11*, 170−175.
(14) Hahm, J.-I.; Lieber, C. M. *Nano Lett.* **2004**, *4*, 51−54.
(15) Li, Z.; Chen, Y.; Li, X.; Kamins, T. I.; Nauka, K.; Williams, R. S. *Nano Lett.* **2004**, *4*, 245−247.
(16) Li, Z.; Rajendran, B.; Kamins, T. I.; Li, X.; Chen, Y.; Williams, R. S. *Appl. Phys. A: Mater. Sci. Process.* **2005**, *80*, 1257−1263.
(17) Gao, Z.-Q.; Agarwal, A.; Trigg, A. D.; Singh, N.; Fang, C.; Tung, C.-H.; Fan, Y.; Buddharaju, K. D.; Kong, J.-M. *Anal. Chem.* **2007**, *79*, 3291−3297.
(18) Bunimovich, Y. L.; Shin, Y. S.; Yeo, W.-S.; Amori, M.; Kwong, G.; Heath, J. R. *J. Am. Chem. Soc.* **2006**, *128*, 16323−16331.
(19) Zhang, G.-J.; Zhang, G.; Chua, J. H.; Chee, R. E.; Wong, E. H.; Agarwal, A.; Buddharaju, K. D.; Singh, N.; Gao, Z. Q.; Balasubramanian, N. *Nano Lett.* **2008**, *8*, 1066−1070.
(20) Cattani-Scholz, A.; Pedone, D.; Dubey, M.; Neppl, S.; Nickel, B.; Feulner, P.; Schwartz, J.; Abstreiter, G.; Tornow, M. *ACS Nano* **2008**, *2*, 1653−1660.
(21) Zhang, G.-J.; Chua, J. H.; Chee, R. E.; Agarwal, A.; Wong, S. M.; Buddharaju, K. D.; Balasubramanian, N. *Biosens. Bioelectron.* **2008**, *23*, 1701−1707.
(22) Zhang, G.-J.; Chua, J. H.; Chee, R. E.; Agarwal, A.; Wong, S. M. *Biosens. Bioelectron.* **2009**, *24*, 2504−2508.
(23) Zhang, G.-J.; Luo, Z. H. H.; Huang, M. J.; Tay, G. K.; Lim, E.-J. *Biosens. Bioelectron.* **2010**, *25*, 2447−2453.
(24) Zhang, G.-J.; Zhang, L.; Huang, M. J.; Luo, Z. H. H.; Tay, G. K.; Lim, E.-J.; Kang, T. G.; Chen, Y. *Sens. Actuators, B* **2010**, *146*, 138−144.
(25) Gao, A.; Lu, N.; Dai, P.; Li, T.; Pei, H.; Gao, X.; Gong, Y.; Wang, Y.; Fan, C. *Nano Lett.* **2011**, *11*, 3974−3978.
(26) Zheng, G.; Patolsky, F.; Cui, Y.; Wang, W. U.; Lieber, C. M. *Nat. Biotechnol.* **2005**, *23*, 1294−1301.
(27) Stern, E.; Klemic, J. F.; Routenberg, D. A.; Wyremebak, P. N.; Turner-Evans, D. B.; Hamilton, A. D.; LaVan, D. A.; Fahmy, T. M.; Reed, M. A. *Nature* **2007**, *445*, 519−522.
(28) Chua, J.; Chee, R. E.; Agarwal, A.; Wong, S. M.; Zhang, G.-J. *Anal. Chem.* **2009**, *81*, 6266−6271.
(29) Lin, T. W.; Hsieh, P. J.; Lin, C. L.; Fang, Y. Y.; Yang, J. X.; Tsai, C. C.; Chiang, P. L.; Pan, C. Y.; Chen, Y. T. *Proc. Natl. Acad. Sci. U.S.A.* **2010**, *107*, 1047−1052.
(30) Zhang, G.-J.; Luo, Z. H. H.; Huang, M. J.; Ang, J. A. J.; Kang, T. G.; Ji, H. M. *Biosens. Bioelectron.* **2011**, *28*, 459−463.
(31) Zhang, G.-J.; Chai, T. C. K.; Luo, Z. H. H.; Huang, M. J.; Tay, G. K. I.; Lim, E.-J. A.; Je, M. *Biosens. Bioelectron.* **2012**, *35*, 218−223.
(32) Patolsky, F.; Zheng, G.; Hayden, O.; Lakadamyali, M.; Zhuang, X.; Lieber, C. M. *Proc. Natl. Acad. Sci. U.S.A.* **2004**, *101*, 14017−14022.
(33) Zhang, G.-J.; Huang, M.; Luo, Z. H. H.; Tay, G. K.; Lim, E.-J.; Liu, E. T.; Thomsen, J. S. *Biosens. Bioelectron.* **2010**, *26*, 365−370.
(34) Zhang, G.-J.; Huang, M.; Ang, J.; Liu, E. T.; Desai, K. V. *Biosens. Bioelectron.* **2011**, *26*, 3233−3239.
(35) Patolsky, F.; Timko, B. P.; Yu, G.; Fang, Y.; Greytak, A. B.; Zheng, G.; Lieber, C. M. *Science* **2006**, *313*, 1100−1104.
(36) Tian, B.; Cohen-Karni, T.; Qing, Q.; Duan, X.; Xie, P.; Lieber, C. M. *Science* **2010**, *329*, 831−834.
(37) Park, I.; Li, Z.; Li, X.; Pisano, A. P.; William, R. S. *Biosens. Bioelectron.* **2007**, *22*, 2065−2070.
(38) Mao, S.; Yu, K. H.; Lu, G. H.; Chen, J. H. *Nano Res.* **2011**, *4*, 921−930.
(39) Mao, S.; Lu, G. H.; Yu, K. H.; Bo, Z.; Chen, J. H. *Adv. Mater.* **2010**, *22*, 3521−3526.
(40) Mao, S.; Lu, G. H.; Yu, K. H.; Chen, J. H. *Carbon* **2010**, *48*, 479−486.
(41) Zhang, G.-J.; Ning, Y. *Anal. Chim. Acta* **2012**, *749*, 1−15.
(42) Lee, M.-r.; Shin, I. *Org. Lett.* **2005**, *7*, 4269−4272.
(43) Svensson, C.; Teneberg, S.; Nilsson, C. L.; Kjellberg, A.; Schwarz, F. P.; Sharon, N.; Krengel, U. *J. Mol. Biol.* **2002**, *321*, 69−83.
(44) Hone, D. C.; Haines, A. H.; Russell, D. A. *Langmuir* **2003**, *19*, 7141−7144.
(45) Szunerits, S.; Niedziołka-Jönsson, J.; Boukherroub, R.; Woisel, P.; Baumann, J. S.; Siriwardena, A. *Anal. Chem.* **2010**, *82*, 8203−8210.
(46) Gruber, K.; Horlacher, T.; Castelli, R.; Mader, A.; Seeberger, P. H.; Hermann, B. A. *ACS Nano* **2011**, *5*, 3670−3678.